2) Most experimental approaches to the neurophysiological problem of measuring alteration of the EEG would employ time-series analysis to detect changes in EEG. Such methods as auto-power and cross-power spectral density analysis are extremely sensitive extractors of signal from noise. It is just this condition that would capitalize on low-level systematic signals that arise from demodulation artifact.

3) The only way to insure a high level of confidence in the results of such an experiment is to demonstrate, in conditions that maximize its detection, the absence of demodulation artifact.

The thermal performance would appear to be limited to, at best, a 1/2°C heating in a 50-mW/cm² field for exposure periods longer than 30–60 s. This is somewhat disappointing, especially, since the ultrahigh-resistance line (bifilament) solved the thermal-diffusion problem. We cannot offer a good explanation of why the bifilament caused the microline to heat.[9] The BeO_2 heat sink would offer some promise for short-exposure durations. If forced air were employed, the length of exposure could be increased to thermal equilibrium, but then the question of removing heat from the brain, skull, and scalp must be considered.

Possible future approaches would include microline that has higher resistance or is longer or both, along with reduced surface area for the platinum transducer pads. Heat sinking and more thermal mass probably offer little promise, since they only seem to delay the eventual development of problems.

This discussion may show a deficiency of the model used for thermal testing; that is, the heat capacity of the head phantom is limited, due to the absence of cerebral circulation. Further, the thermal gradients are unrealistic in the model as compared to a real head. For example, in the model the phantom begins at uniform temperature, whereas in the head, deep brain is warmer than surface brain, and both are warmer than the skull and scalp. In other words, the 1/2°C heating at the electrode needle may represent an extreme that could be reduced if the model were improved to include more realistic thermal gradients and thermodynamics. Of course, these arguments could be applied to the nondecoupled electrode as well. The issue is merely that, in its present state, the thermodynamics of the phantom are more rigorous than those of the animal. In other words, the phantom provides for a dosimetric mapping of fields within a target; it does not model thermoregulation. Nevertheless, the present electrode does modify power absorption, although the perturbation it introduces is much reduced in comparison to that associated with conventional conductors (cf. [1], [5]).

CONCLUSION

The 5-μm MIC electrode is free from demodulation artifact (as detectable in the PSD) at power densities up to 100 mW/cm². Conventional electrodes of small surface area (5-mil diameter W wire) demodulated at 5 mW/cm². The MIC electrode and monofilament with BeO_2 heat sink heated less than 0.1°C for the first 30–60 s of exposure in a 50-mW/cm² field. After several minutes of exposure, when thermal equilibrium is established, the electrode heats about 0.6°C. Ultrahigh-resistance line (bifilament) reduced lead heating and thermal diffusion to negligible proportions but enhanced needle heating.

ACKNOWLEDGMENT

The authors wish to thank P. E. Shoaf for his technical assistance.

REFERENCES

[1] L. E. Larsen, R. A. Moore, and J. Acevedo, "A microwave decoupled brain-temperature transducer," *IEEE Trans. Microwave Theory Tech.*, vol. MTT-22, pp. 438–444, Apr. 1974.
[2] R. Elul, "Dipoles of spontaneous activity in the cerebral cortex," *Exp. Neurol.*, vol. 6, pp. 285–299, 1962.
[3] L. E. Larsen, "Brain temperature and EEG data acquisition from animals during microwave exposure," in *Dig. Papers, Joint U. S. Army/Georgia Inst. of Tech. Microwave Dosimetry Workshop*, 1972, pp. 4–9.
[4] A. W. Guy, "Analyses of electromagnetic fields induced in biological tissues by thermographic studies on equivalent phantom models," *IEEE Trans. Microwave Theory Tech. (Special Issue on Biological Effects of Microwaves)*, vol. MTT-19, pp. 205–214, Feb. 1971.
[5] J. F. Lehmann, A. W. Guy, B. J. Delateur, J. P. Stonebridge, and C. G. Warren, "Heating patterns produced by short wave diathermy using helical coil applicators," *Arch. Phys. Med. Rehabil.*, vol. 49, pp. 193–198, 1968.

[9] Currents in the microline are not transmitted without loss to the brain interface due to an impedance discontinuity at the pad-microline junction. Fringe effects from the edge thickness of the pads may be troublesome, but the 40–60-mil spot size of spatial resolution for the thermograph can detect all but the smallest of thermal point sources from the 20 mils of combined pad dimension.

Error in Impedance Measurement When the Signal is Introduced Across the Slotted-Line Probe

JESÚS BARBERO

***Abstract*—For some special applications impedance measurements have to be made where the test level reaching the unknown must be kept very low. In such cases, using slotted-line techniques, the detector and generator are reversed in the test setup, and the test signal is introduced across the probe of the slotted line which is terminated on one side with the load, and on the other with the detector. This short paper briefly describes this familiar method and then discusses the error calculation in the measurement of VSWR and phase when the detector is not perfectly matched.**

I. INTRODUCTION

The classical impedance measurement with the slotted line needs a signal level strong enough to excite a meter after detection. Nevertheless, when the signal level reaching the unknown must be kept very low (e.g., as is the case of active element measurements) it happens that the available energy is insufficient to excite the meter, even a standing wave ratio meter. In such cases, it is possible to change around the generator and detector [1]–[3], introducing the signal across the slotted-line probe. With this arrangement, an increase in sensitivity results because detection is carried out using the signal level right in the line and not across the coupling of the probe where the signal is weaker. Another advantage of this arrangement is that it is possible to work with a well-decoupled probe, because we are only limited by the power that we can get from the generator to have the desired level in the line. In this way the influence of the probe on the measurement is avoided.

If the detector is not perfectly matched, the incident signal on it will be partially reflected and will add vectorially with the excited wave in the probe plane. So the incident wave in the load depends on detector reflection coefficient and on probe position.

In this short paper, the possible errors in the VSWR and in the phase measurement as a function of detector mismatch are calculated so that it is possible to determine the accuracy with which the detector must be matched depending on the desired precision of the measurement.

II. FORMULATION OF THE PROBLEM

Let us consider the two parallel lines as in Fig. 1. In this figure x and y are the distances to probe plane AA', variables with probe displacement, but always keeping $x + y = l$ (l being the electric distance between load and detector).

As it has already been stated, we can work with a well-decoupled probe and so the electromagnetic state of the line will not influence the generator nor, consequently, the excitation voltage. Thus, in each line (X or Y), the incident wave, i.e., the propagating wave in the positive sense (OX or OY), will be the vectorial addition of the excited wave by the probe and the reflected wave arriving from the other line (Y or X). So we can only consider one incident wave and one reflected wave and they are related by the reflection coefficients Γ_x and Γ_D.

Thus, with the foregoing considerations using basic transmission-line theory [4]–[6], we can write

$$V(-y) = V_{y1} \exp(j\beta y) + V_{y2} \exp(-j\beta y)$$
$$V(-x) = V_{x1} \exp(j\beta x) + V_{x2} \exp(-j\beta x) \quad (1)$$

$$\Gamma_x = |\Gamma_x| \exp(j\psi) = \frac{V_{x2}}{V_{x1}} \quad (2)$$

$$\Gamma_D = |\Gamma_D| \exp(j\varphi) = \frac{V_{y2}}{V_{y1}} \quad (3)$$

$$V_{x1} \exp(j\beta x) = V + V_{y2} \exp(-j\beta y) \quad (4)$$

$$V_{y1} \exp(j\beta y) = V + V_{x2} \exp(-j\beta x) \quad (5)$$

Manuscript received January 21, 1974; revised March 11, 1974.
The author is with the Centro de Investigaciones Fisicas, Serrano, 144, Madrid, 6, Spain.

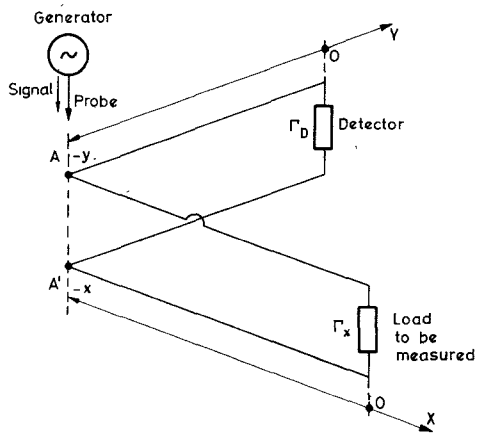

Fig. 1. Equivalent circuit of test setup with reversed position of generator and detector.

$$x + y = l \tag{6}$$

where V_{y1}, V_{y2}, V_{x1}, and V_{x2} are complex constants; $j\beta$ represents the propagation constant (line without losses); Γ_D and Γ_x represent, respectively, the reflection coefficient of the detector and of the load to be measured; and V is the voltage excited by the probe in the line (complex constant).

From the resolution of system (1)–(6) we obtain

$$V(-x) = V\{1 + |\Gamma_x| \exp[j(\psi - 2\beta x)]\} \cdot (1 + \Delta\{|\Gamma_x| + \exp[-j(\psi - 2\beta x)]\}) \tag{7}$$

where

$$\Delta = \frac{|\Gamma_D| \exp[j(\varphi + \psi - 2\beta l)]}{1 - |\Gamma_x||\Gamma_D| \exp[j(\varphi + \psi - 2\beta l)]}. \tag{8}$$

It should be noted that Δ is independent of probe position, and it depends only on detector (Γ_D), on the load to be measured (Γ_x), on the electric distance between them (l), and on the phase constant, i.e., wavelength ($\beta = 2\pi/\lambda$).

Nevertheless, it is impossible to know Δ because of its relation to Γ_x, which is the unkown. This is the reason why we have determined the boundaries of measured VSWR as a function of detector mismatch.

III. UPPER LIMIT OF MEASURED VSWR

In (7) we can see that for each Δ there is a maximum and a minimum of $V(-x)$. When Δ is real positive and the greatest ($\Delta = |\Delta_{\max}|$ for $\varphi + \psi - 2\beta l = 2k\pi$) we will obtain the maximum of maxima of $|V(-x)|$ ($|V_{MM}|$) for $\psi - 2\beta x = 2k\pi (k = 0,1,2,\cdots)$ and the minimum of minima ($|V_{mm}|$) for $\psi - 2\beta x = (2k+1)\pi$. And the upper limit of measured VSWR (σ_{xM}) will be

$$\sigma_{xM} = \frac{|V_{MM}|}{|V_{mm}|} = \frac{1 + |\Gamma_x|}{1 - |\Gamma_x|} \cdot \frac{1 + |\Gamma_D|}{1 - |\Gamma_D|} = \sigma_x \cdot \sigma_D \tag{9}$$

σ_x and σ_D being, respectively, the actual VSWR of load and detector.

IV. LOWER LIMIT OF MEASURED VSWR

In a similar way, as in the previous section, we must now find the minimum of maxima ($|V_{mM}|$) and the maximum of minima ($|V_{Mm}|$) of $|V(-x)|$. Always $\Delta > -|\Delta_{\max}|$, and so the lower limit of measured VSWR (σ_{xm}) will be

$$\sigma_{xm} = \frac{|V_{mM}|}{|V_{Mm}|} > \sigma_x \cdot \frac{1}{\sigma_D} \cdot \frac{1 - 2|\Gamma_x||\Gamma_D| - |\Gamma_D|^2(1 + 2|\Gamma_x|)}{1 - 2|\Gamma_x||\Gamma_D| - |\Gamma_D|^2(1 - 2|\Gamma_x|)} \tag{10}$$

and for small values of $|\Gamma_D|$

$$\sigma_{xm} > \sigma_x \cdot \frac{1}{\sigma_D}.$$

It should be observed that the lower limit given by (10) is impossible to reach no matter the value of $\varphi + \psi - 2\beta l$. On the contrary, the upper limit given by (9) can be reached when $\varphi + \psi - 2\beta l = 2k\pi (k = 0,1,2,\cdots)$.

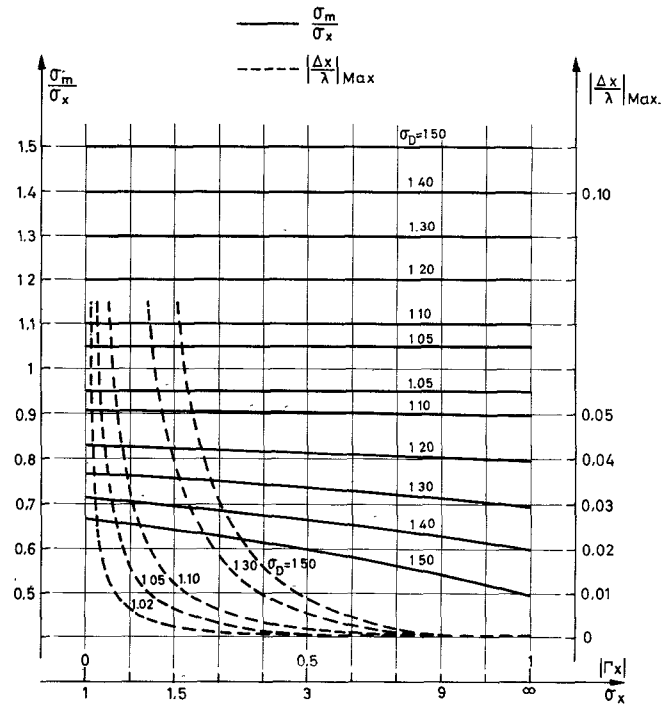

Fig. 2. Error in VSWR and phase measurement versus reflection coefficient ($|\Gamma_x|$), with detector VSWR (σ_D) as a parameter.

In Fig. 2 the solid lines represent the computation of expressions (9) and (10). For each σ_D, the upper limit of σ_m/σ_x will be the corresponding line above $\sigma_m/\sigma_x = 1$ and the lower limit the corresponding line below $\sigma_m/\sigma_x = 1$ (σ_m is the measured VSWR). When $\sigma_D = 1$ (matched detector), the measured VSWR is the actual VSWR of the load as expected.

V. PHASE ERROR

The conditions for minimum of function $|V(-x)|^2$ are:

$$|\Gamma_x|(1 + |\Gamma_D|^2)\sin\alpha + |\Gamma_D|(1 + |\Gamma_x|^2)\sin(\alpha - \gamma) + 2|\Gamma_x||\Gamma_D|\sin(2\alpha - \gamma) = 0 \tag{11}$$

$$|\Gamma_x|(1 + |\Gamma_D|^2)\cos\alpha + |\Gamma_D|(1 + |\Gamma_x|^2)\cos(\alpha - \gamma) + 4|\Gamma_x||\Gamma_D|\cos(2\alpha - \gamma) < 0 \tag{12}$$

where $\psi - 2\beta x = \alpha$ and $\varphi + \psi - 2\beta l = \gamma$.

Resolution of (11) with condition (12) is very easy with a computer. We can see that the value of α will depend on γ which depends on electric distance between load and detector, on frequency, and on the reflection coefficient phases of load and detector. Being that the value of γ cannot be determined, we must resort to calculating the maximum error, i.e., the maximum deviation from ideal position of minimum (as we have seen in Section III, ideal position of minimum corresponds to $\psi - 2\beta x = (2k+1)\pi$).

The results obtained with a computer are shown in Fig. 2 with dashed lines, where $|\Delta x/\lambda|_{\max}$ is the maximum deviation (relative to λ) of the ideal position of minimum.

VI. CONCLUSIONS

The solid lines in Fig. 2 show that for precision measurements good matching of detector is necessary. A usual VSWR of commercial detectors (e.g., 1.30 or 1.50) makes the measurement useless. Error is almost independent of load VSWR (σ_x) at least for weak σ_D.

The dashed lines in this figure show that error in phase depends very much on load VSWR (σ_x), and for near short-circuit conditions (even for $\sigma_x \simeq 6$) the error is small. But for small values of σ_x the error may be very important. It is evident that for values of σ_x very near to unity, phase error is of no concern, but between matched load and short-circuit conditions there are values of σ_x where phase error can be very important if the detector is not well matched.

To perform precision measurements, the detector must be matched beforehand. These measurements may be accomplished by matching the detector using a slotted line in the conventional mode of opera-

tion. To avoid the possibility of variation of detector impedance with signal level, the detector can be preceded by a ferrite isolator or an attenuator. In the latter case the sensitivity will be lower, but the author has obtained good results in varactor-diode measurements operating in this manner.

ACKNOWLEDGMENT

The author wishes to thank R. Freeman of ITT Laboratories in Madrid for his help in the composition of this short paper.

REFERENCES

[1] E. L. Ginzton, *Microwave Measurements*. New York: McGraw-Hill, 1957, p. 307.
[2] L. A. Blackwell and K. L. Kotzebue, *Semiconductor-Diode Parametric Amplifiers*. Englewood Cliffs, N. J.: Prentice-Hall, 1961, p. 138.
[3] H. M. Altschuler, "The interchange of source and detector in low-power microwave network measurements," *IEEE Trans. Microwave Theory Tech. (1964 Symposium Issue)*, vol. MTT-13, pp. 84–90, Jan. 1965.
[4] G. L. Ragan, *Microwave Transmission Circuits*. New York: McGraw-Hill, 1948, ch. 2.
[5] H. H. Skilling, *Electric Transmission Lines*. New York: McGraw-Hill, 1951, ch. 1.
[6] R. I. Sarbacher and W. A. Edson, *Hyper and Ultrahigh Frequency Engineering*. New York: Wiley, 1943, ch. 9.

Multilayer Microstrip Transmission Lines

ANDREW FARRAR, MEMBER, IEEE, AND A. T. ADAMS, SENIOR MEMBER, IEEE

***Abstract*—A method used to treat covered microstrip is extended to multilayer microstrip. Detailed results are obtained for the general three-layer problem. Series expansion and term-by-term integration are used to obtain a closed form expression for the Green's function. Matrix methods are then used to obtain the characteristic impedance. Data obtained agree closely with experiment.**

I. INTRODUCTION

Multilayer microstrip (see Fig. 1) is often used in the design of microstrip components which operate at high levels of RF power (kilowatt) or in the design of overlay microwave couplers. Hence there is a need for the basic design data for multilayer microstrip. Yamashita and Atsuki [5], [6] have treated multilayer microstrip problems by variational methods. The method of separation of variables has previously been used in the derivation of the Green's function for covered microstrip [1]. In this short paper the formulation is extended to obtain the potential distribution for multilayer microstrip in general form. The general solution for the Green's function may be completed by the inversion of an N by N matrix, where N is the number of layers, and the evaluation of an infinite integral. Once the Green's function is obtained, then the electrostatic properties of multilayer–multiconductor microstrip, such as the capacitance matrix, may be obtained by matrix methods [2], [3]. The characteristics of quasi-TEM propagation may then be approximately calculated.

Specific results are obtained for the three-layer problem. The infinite integral is evaluated by series expansion and term-by-term integration, to obtain a closed form expression for the Green's function (potential due to a line charge in three-layer microstrip). A general computer program has been written for three-layer microstrip. Results obtained by the program agree well with experiment (to within a few percent).

II. N-LAYER MICROSTRIP

Consider the microstrip shown in Fig. 1. The Green's function for this problem is derived by considering a line of charge residing on the

Manuscript received February 15, 1974; revised April 15, 1974.

A. Farrar is with the Heavy Military Electronics Systems Division, General Electric Company, Syracuse, N. Y. 13201.
A. T. Adams is with the Electrical and Computer Engineering Department, Syracuse University, Syracuse, N. Y. 13210.

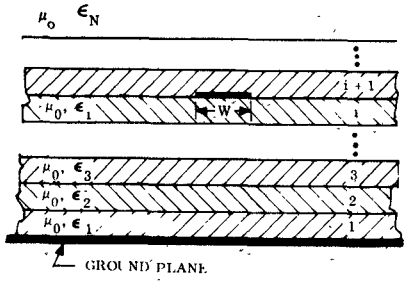

Fig. 1. Microstrip with N-layer dielectric.

ith boundary (Fig. 2). The potential V in each layer of dielectric is given by the solution of Laplace's equation

$$\nabla^2 V = 0 \tag{1}$$

which has a solution of the form

$$V = (A \sin kx + B \cos kx)(C \sin hky + D \cos hky). \tag{2}$$

Specializing the solution to the problem in Fig. 2 one can write

$$\begin{aligned}
V_1 &= \int_{-\infty}^{\infty} \cos kx (a_1 \sin hky)\, dk \\
V_2 &= \int_{-\infty}^{\infty} \cos kx (a_2 \sin hky + b_2 \cos hky)\, dk \\
&\vdots \\
V_i &= \int_{-\infty}^{\infty} \cos kx (a_i \sin hky + b_i \cos hky)\, dk \\
&\vdots \\
V_N &= \int_{-\infty}^{\infty} \cos kx a_N \exp(-ky)\, dk
\end{aligned} \tag{3}$$

where the subscript $1,2,\cdots,N$ refers to the dielectric layers $1,2,\cdots,N$. The coefficients $a_1,a_2,a_3,\cdots,a_N$ and $b_2,b_3,\cdots$, and b_{N-1} are evaluated using the following boundary conditions at the interfaces:

$$V_i = V_{i+1} \tag{4}$$

$$D_i - D_{i+1}\,|_{y=d_i} = \sigma_i = \lambda_i \delta(x)$$

where the subscript i refers to the ith layer of the dielectric where the charge is located. Substituting (3) into (4) the result in matrix form may be written as

$$\begin{bmatrix}
S_1 & -S_1 & -C_1 & \cdot & \cdot & \cdot & \cdot & 0 & 0 \\
\epsilon_1 C_1 & -\epsilon_2 C_1 & -\epsilon_2 S_1 & \cdot & \cdot & \cdot & \cdot & & \\
\cdot & \cdot & \cdot & & & & & & \\
\cdot & \cdot & \cdot & & & & & & \\
\cdot & \cdot & \cdot & & & & & & \\
0 & & & S_i & C_i & -S_i & -C_i & \cdots & 0 \\
0 & & & \epsilon_i C_i & \epsilon_i S_i & -\epsilon_{i+1} C_i & -\epsilon_{i+1} S_i & \cdots & 0 \\
\cdot & \cdot & \cdot & & & & & & \\
\cdot & \cdot & \cdot & & & & & & \\
\cdot & \cdot & \cdot & & & & & & \\
0 & 0 & 0 & \cdot & \cdot & \epsilon_{N-1} C_{N-1} & \epsilon_{N-1} S_{N-1} & e_N e^{-kd_{N-1}} &
\end{bmatrix}$$

$$\times \begin{bmatrix} a_1 \\ \cdot \\ \cdot \\ \cdot \\ a_i \\ b_i \\ b_{N-1} \\ a_N \end{bmatrix} = \begin{bmatrix} 0 \\ 0 \\ \cdot \\ \cdot \\ \cdot \\ 0 \\ \lambda \\ \hline 2\pi k \\ \cdot \\ \cdot \\ \cdot \\ 0 \end{bmatrix} \tag{5}$$